

Learning when to rank: Estimation of partial rankings from sparse, noisy comparisons

Sebastian Morel-Balbi^{1,*} and Alec Kirkley^{1,2,3,†}

¹*Institute of Data Science, University of Hong Kong, Hong Kong*

²*Department of Urban Planning and Design, University of Hong Kong, Hong Kong*

³*Urban Systems Institute, University of Hong Kong, Hong Kong*

A common task arising in various domains is that of ranking items based on the outcomes of pairwise comparisons, from ranking players and teams in sports to ranking products or brands in marketing studies and recommendation systems. Statistical inference-based methods such as the Bradley Terry model, which extract rankings based on an underlying generative model of the comparison outcomes, have emerged as flexible and powerful tools to tackle the task of ranking in empirical data. In situations with limited and/or noisy comparisons, it is often challenging to confidently distinguish performance of different items based on the evidence available in the data. However, existing inference-based ranking methods overwhelmingly choose to assign each item to a unique rank or score, suggesting a meaningful distinction when there is none. Here we address this problem by developing a principled Bayesian methodology for learning partial rankings—rankings with ties—that distinguishes among the ranks of different items only when there is sufficient evidence available in the data. Our framework is adaptable to any statistical ranking method in which the outcomes of pairwise observations depend on the ranks or scores of the items being compared. We develop a fast agglomerative algorithm to perform Maximum A Posteriori (MAP) inference of partial rankings under our framework and examine the performance of our method on a variety of real and synthetic network datasets, finding that it frequently gives a more parsimonious summary of the data than traditional ranking, particularly when observations are sparse.

I. INTRODUCTION

In a broad range of applications it can be useful to rank a set of items or players according to some predetermined notion of importance or strength. For example, rankings of players or teams, such as FIFA rankings in soccer or Elo ratings in chess, are used to determine match pairings and tournament seedings. Search engines rank web pages so as to deliver the most relevant results to users. In market analytics, products are often ranked based on sales, reviews, and customer satisfaction. In academia, research funding is often allocated by ranking grant applications, while in finance, credit scoring ranks individuals by creditworthiness, significantly influencing their access to loans, mortgages, and other financial services.

Given the prominence of rankings across domains, it has long been of interest to develop algorithms that automatically rank items based on some set of data about each item [1, 2]. An extensively studied subset of ranking problems is that of ranking from *pairwise comparisons* [3–6], where rankings are inferred from comparisons among pairs of entities. In this approach, the outcome of a single interaction between two items—for example, a win or loss in sports or one product being preferred over another—serves as the basis for the ranking. This approach allows one to infer rankings in situations where underlying ratings of the entities are unavailable, unobserved, or difficult to compute. For example, instead of trying to assess the absolute skill of individual tennis players, we can infer their relative rankings from their

head-to-head match results, assuming that matches are more often won by the better player.

Since pairwise comparisons inherently involve some degree of uncertainty due to randomness, noise, or incomplete information in the observed outcomes, pairwise ranking models are generally formulated as probabilistic models whose parameters can then be estimated, for example, via Maximum Likelihood Estimation (MLE) or Maximum A Posteriori (MAP) inference [5, 7–10]. It is also useful to model pairwise comparison data as a network in which items are nodes and each comparison is an edge between its participating nodes, pointing from the winner of the corresponding match/preferred item to the loser of the match/non-preferred item. Multiple edges may exist between a pair of nodes if multiple comparisons were performed, each edge providing evidence for the relative ranking of the two items on its endpoints.

In the classic Bradley Terry model [5], the outcome of a comparison between two nodes is modeled as a Bernoulli random variable with a probability that depends on the latent scores associated with the items. After inference with the model, one obtains a set of continuous scores that can be ordered to obtain a final ranking. The Bradley Terry model has inspired numerous extensions [6, 11] to more flexibly model variations in match outcomes, including the possibility of ties in the match outcomes [12–15] (rather than ties in the final *rankings* as we study here). Another popular inference-based method for ranking from pairwise comparisons is SpringRank [9], which ranks nodes by finding the ground state of a physical system which models the comparison network as a set of directed springs and has also inspired numerous generalizations [16, 17]. These methods can parsimoniously model heterogeneity and noise in match outcomes but do

* sebastian.morel@gmail.com

† alec.w.kirkley@gmail.com

not allow for the possibility of ties in the inferred rankings, and, as such, are unable to determine when there is enough structure in the comparison data to justify distinguishing the rankings of different items. (In principle, two players can have identical scores under such methods, but this is rarely ever achieved in practice numerically.) Such methods can therefore infer rankings that overfit the data when limited observations are available, resulting in rankings that are highly sensitive to small changes in outcomes. In the ordered Stochastic Block Model (OSBM) of Peixoto [10], nodes are grouped according to both the mixing structure of the network and hierarchies among the nodes as evidenced by edge directionality. Although the OSBM does allow nodes to be grouped in part by the edge hierarchy, it is heavily influenced by the mixing structure of the nodes, which largely depends on the positions of the edges rather than their directionality (the latter aspect being of primary interest for pairwise ranking). In contrast, the method we propose here focuses only on the directionality of the observed edges and so is adaptable to a broad class of ranking methods, including most popular generalizations of the Bradley-Terry model [6].

In this work we introduce a statistical inference-based ranking framework that intrinsically incorporates partial rankings—rankings where multiple nodes can have the same rank—into its underlying generative model. This is accomplished by introducing a hierarchy of uniform Bayesian priors for the underlying rankings of the nodes, which encourages parsimony in the final scores or ranks inferred using the model. This allows us to account for the uncertainty introduced by sparsity in the data by grouping players into the same rank when the data does not provide enough evidence to separate them. Furthermore, our method can be extended to accommodate any inference-based ranking method that models comparison outcomes as a function of the underlying scores or ranks of the nodes involved [5, 6, 9]. We provide a fast nonparametric agglomerative algorithm to infer the partial rankings according to our method, and by fitting our model to a wide range of synthetic and real-world datasets, we find that it often provides a more parsimonious description of the data in the regime of sparse observations. As a case study, we apply our method to a faculty hiring network among Computer Science departments at US universities [18]. The picture that emerges is that of a well-separated hierarchy dominated by a small group of elite universities whose rankings are not meaningfully different statistically, with very little upward mobility across the ranking groups.

The paper is organised as follows. In Sec. II, we introduce the Bradley-Terry model, our partial rankings model, and the agglomerative algorithm we use to perform MAP inference with our model. In Sec. III A and Sec. III B, we apply our method to a wide range of synthetically generated datasets as well as a corpus of empirical networks, finding that partial rankings can provide a more parsimonious description of the data in cases where

the networks of outcomes are not sufficiently dense. In Sec. III C, we focus on a network of faculty hiring among computer science departments in the U.S. and show that our algorithm can be used to extract meaningful ambiguities in the rankings of these departments. We finalize in Sec. IV with our conclusions.

II. METHODS

A. Bayesian Ranking and the Bradley-Terry Model

For illustrative purposes, it will be convenient to discuss ranking in the context of matches among individuals—for example, tennis matches among tennis players. But all upcoming discussion can be equivalently framed in the context of comparing two items, in which case each match is a comparison (e.g. from a respondent in a marketing survey or a consumer purchasing one of multiple products), and the winner of the match is the preferred item.

Let \mathbf{W} be an $N \times N$ matrix of match outcomes for a set of N competing individuals (nodes) such that w_{ij} is the number of matches in which node i beat node j . For simplicity, we will assume that ties in the matches are not allowed. The problem we want to solve is that of inferring a ranking $\mathbf{r} = [r_1, \dots, r_N]$ of the N individuals such that $r_i < r_j$ indicates a higher probability of i beating j than j beating i . Given the inherently probabilistic nature of match outcomes, a common approach is to assign a latent real-valued score $s_i \in \mathbb{R}$ to each player such that the probability p_{ij} that player i beats player j is given by some function of the difference of their scores: $p_{ij} = f(s_i - s_j)$. For $f(s)$ to be a suitable scoring function, it must satisfy a set of constraints [6]: (1) It must be a monotonically increasing function of s , ensuring that stronger players are assigned a higher probability of winning; (2) It must be bounded within $[0, 1]$ as it must represent a valid probability; (3) It must be antisymmetric around zero, satisfying $f(-s) = 1 - f(s)$ to ensure that the probability of losing is one minus the probability of winning. While these requirements do not uniquely determine $f(s)$, a commonly adopted choice is the logistic function, $f(s) = 1/(1 + e^{-s})$, which gives

$$p_{ij} = \frac{e^{s_i}}{e^{s_i} + e^{s_j}}. \quad (1)$$

For convenience, one generally introduces the quantities $\pi_i = e^{s_i}$, which, keeping with previous literature, we shall call the player *strengths* [19, 20]. Eq. 1 can then be written as

$$p_{ij} = \frac{\pi_i}{\pi_i + \pi_j}. \quad (2)$$

This win probability is the basis of the well known Bradley-Terry (BT) model, first introduced by Zermelo [19] and then, independently, by Bradley and Terry [5].

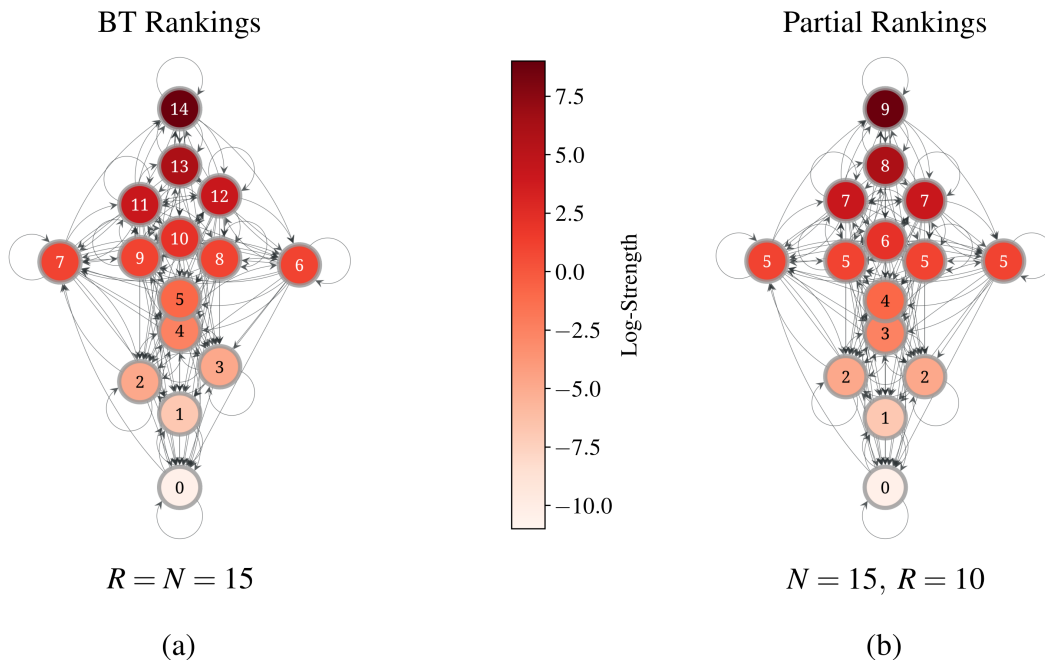


FIG. 1. **Partial rankings in a small example network.** (a) Rankings inferred by the Bradley-Terry model and (b) the partial rankings algorithm, for a dataset capturing hierarchical relationships in a pack of wolves. The nodes are labeled according to their inferred ranking. The distance along the y-axis and the node colors are proportional to the inferred strength π_i of each node i , with the strongest nodes placed at the top. In this case, there was not enough statistical evidence in the edges to justify separating the node ranks $\{2, 3\}$, $\{6, 7, 8, 9\}$, and $\{11, 12\}$ on the left hand side, so the partial ranking method grouped these nodes together into the same partial rankings.

Given the matrix \mathbf{W} and assuming all match outcomes are independent of each other, the likelihood of observing \mathbf{W} is given by

$$P(\mathbf{W}|\boldsymbol{\pi}) = \prod_{ij} \left(\frac{\pi_i}{\pi_i + \pi_j} \right)^{w_{ij}}. \quad (3)$$

Allowing the gradient with respect to $\boldsymbol{\pi}$ to vanish gives a self-consistent set of equations for the Maximum Likelihood estimates of the scores. Then, these scores are converted to an implied ranking \mathbf{r} by simply taking the ordering of the nodes with respect to the inferred strengths $\boldsymbol{\pi}$ [5, 19–21].

Note that Eq. 2, and therefore Eq. 3, is invariant under a constant rescaling of all player strengths. To resolve this ambiguity, one generally imposes a suitable normalisation. A common choice is to fix the average player score to zero

$$\langle s \rangle = \frac{1}{N} \sum_{i=1}^N s_i = 0. \quad (4)$$

This choice centres the log-strengths around zero, making them interpretable as relative to an average player. In turn, this ensures that the strength of the average player is given by $\langle \pi \rangle = 1$, so that a player with $\pi_i > 1$ is stronger than average, and one with $\pi_i < 1$ is weaker than average. This normalisation choice also has the advantage of providing an intuitive interpretation of the

player’s strengths. Following [20], let p_1 be the probability that a player with strength π has of beating the average player of strength one. Then, according to the Bradley-Terry model, p_1 is given by $p_1 = \pi/(\pi+1)$, which in turn implies that $\pi = p_1/(1-p_1)$. A player’s strength is then simply the odds that the player has of beating the average player.

Maximum Likelihood Estimation (MLE) is not the only method for inferring player strengths. Often a prior $P(\boldsymbol{\pi})$ is placed on the strengths $\boldsymbol{\pi}$ so that a full posterior distribution over $\boldsymbol{\pi}$ can be inferred [1, 2, 20, 22]. A common choice for this prior is to assume a uniform distribution over the probability p_1 that a player with strength π defeats the average player, $P(p_1) = 1$. By probability density transformation rules, this is equivalent to setting a logistic prior on the scores $s_i = \log \pi_i$. Indeed,

$$P(s) = P(p_1) \cdot \frac{dp_1}{ds} = \frac{dp_1}{d\pi} \frac{d\pi}{ds} = \frac{\pi}{(\pi+1)^2} = \frac{e^s}{(1+e^s)^2}, \quad (5)$$

which is a logistic distribution with mean zero and scale one. If we assume the scores of all players to be independently distributed, we have the following prior on the player strengths

$$P(\boldsymbol{\pi}) = \prod_i \frac{\pi_i}{(\pi_i+1)^2}. \quad (6)$$

For this Bayesian model, Maximum A Posteriori (MAP) estimates for $\boldsymbol{\pi}$ can be inferred by solving the following optimisation problem:

$$\hat{\boldsymbol{\pi}} = \arg \max_{\boldsymbol{\pi}} P(\boldsymbol{\pi}|\mathbf{W}) = \arg \max_{\boldsymbol{\pi}} P(\mathbf{W}|\boldsymbol{\pi})P(\boldsymbol{\pi}). \quad (7)$$

Allowing the gradient with respect to $\boldsymbol{\pi}$ to vanish gives a self-consistent set of equations for the MAP estimates $\hat{\boldsymbol{\pi}}$, which can be solved in the same way as for the MLEs. The inferred strengths are then converted into an implied ranking \mathbf{r} by ordering the nodes with respect to the inferred strengths $\hat{\boldsymbol{\pi}}$.

B. Partial Rankings

As discussed in Sec. I, a limitation of standard MAP estimation for the BT model is that it lacks a mechanism to handle partial rankings. In principle, one could apply a heuristic to assign the same rank to nodes i and j when their scores satisfy $|s_i - s_j| < \epsilon$ for some small ϵ . However, this approach does not offer any statistical justification for grouping i and j together (i.e., whether the observed score difference is simply due to statistical noise). Alternatively, one could apply 1D numerical clustering to the final score values, but this approach would not account for the significance of score differences in the context of the model's likelihood or prior.

A principled approach to handling partial rankings in the Bradley-Terry model is to extend the Bayesian hierarchy for the prior on the strengths $P(\boldsymbol{\pi})$ by making the strength of each node a function of its underlying ranking \mathbf{r} . This results in the following new MAP objective:

$$\begin{aligned} \hat{\mathbf{r}}, \hat{\boldsymbol{\pi}} &= \arg \max_{\mathbf{r}, \boldsymbol{\pi}} P(\mathbf{r}, \boldsymbol{\pi}|\mathbf{W}) \\ &= \arg \max_{\mathbf{r}, \boldsymbol{\pi}} P(\mathbf{W}|\boldsymbol{\pi})P(\boldsymbol{\pi}|\mathbf{r})P(\mathbf{r}), \end{aligned} \quad (8)$$

where $\hat{\mathbf{r}}$ represents the optimal partial ranking to be estimated from the observed data and $\hat{\boldsymbol{\pi}}$ is the optimal set of scores, as defined previously.

Given Eq. 8, we now need to define the functional forms of the likelihood and priors. The easiest choice is to use the Bradley-Terry likelihood of Eq. 3, although any choice of likelihood is possible to incorporate into this MAP estimation objective so long as it is a function of latent strengths—i.e., $P(\mathbf{W}|\boldsymbol{\pi})$ —or ranks—i.e., $P(\mathbf{W}|\mathbf{r})$ (the latter allowing us to remove the prior $P(\boldsymbol{\pi}|\mathbf{r})$). This flexibility allows for the inclusion of a wide range of ranking objectives including extensions of Bradley Terry models [6] and SpringRank [9]. For our experiments in Sec. III, we will proceed with using the Bradley Terry likelihood of Eq. 3 for subsequent analysis, which facilitates an efficient optimization scheme and a simple comparison with the original Bradley Terry model.

For the prior on \mathbf{r} , we choose to be agnostic with respect to both the number and sizes of the underlying rankings, This results in a hierarchy of uninformative priors, as described by the following generative model:

1. Draw the number of unique ranks R uniformly at random from the range $[1, N]$.
2. Draw the histogram $\mathbf{n} = [n_1, \dots, n_R]$ of the number of nodes of each rank uniformly from the set of all histograms compatible with the number of ranks R .
3. Draw the ranks \mathbf{r} uniformly over the set of rankings compatible with the rank counts \mathbf{n} .

The resulting prior is then given by

$$\begin{aligned} P(\mathbf{r}) &= P(\mathbf{r}|\mathbf{n})P(\mathbf{n}|R)P(R) \\ &= \frac{1}{\binom{N}{n_1, \dots, n_R}} \times \frac{1}{\binom{N-1}{R-1}} \times \frac{1}{N}. \end{aligned} \quad (9)$$

A reasonable choice for the prior $P(\boldsymbol{\pi}|\mathbf{r})$ is a hierarchical prior consisting of two steps: (1) Draw the set of unique strengths $\boldsymbol{\sigma} = \{\sigma_1, \dots, \sigma_R\}$ based on the number of unique ranks R ; (2) Draw the individual strengths $\boldsymbol{\pi}$ using the deterministic prior $P(\boldsymbol{\pi}|\boldsymbol{\sigma}) = \prod_{i=1}^N \delta(\pi_i, \sigma_{r_i})$. Combining these gives the prior

$$\begin{aligned} P(\boldsymbol{\pi}|\mathbf{r}) &= P(\boldsymbol{\pi}|\boldsymbol{\sigma})P(\boldsymbol{\sigma}|\mathbf{r}) \\ &= \prod_{i=1}^N \delta(\pi_i, \sigma_{r_i}) \prod_{r=1}^R P(\sigma_r) \prod_{r=1}^{R-1} \Theta(\sigma_r - \sigma_{r+1}), \end{aligned} \quad (10)$$

where Θ is the Heaviside step function and $P(\sigma_r)$ is given by

$$P(\sigma_r) = \frac{\sigma_r}{(\sigma_r + 1)^2} \quad (11)$$

as in the Bradley-Terry model.

The MAP estimation objective can now be written as the following minimisation problem in terms of the log posterior

$$\hat{\mathbf{r}}, \hat{\boldsymbol{\sigma}} = \arg \min_{\mathbf{r}, \boldsymbol{\sigma}} [-\log P(\mathbf{r}, \boldsymbol{\pi}(\boldsymbol{\sigma})|\mathbf{W})] \quad (12)$$

$$= \arg \min_{\mathbf{r}, \boldsymbol{\sigma}} \{\mathcal{L}(\mathbf{r}, \boldsymbol{\sigma})\}, \quad (13)$$

where

$$\begin{aligned} \mathcal{L}(\mathbf{r}, \boldsymbol{\sigma}) &= \log N + \log \binom{N-1}{R-1} + \log \binom{N}{n_1, \dots, n_R} \\ &+ \sum_{r=1}^R \log \left[\frac{(\sigma_r + 1)^2}{\sigma_r} \right] + \sum_{r, r'=1}^R \omega_{rr'} \log \left[\frac{\sigma_r + \sigma_{r'}}{\sigma_r} \right], \end{aligned} \quad (14)$$

with

$$\omega_{rr'} \equiv \sum_{ij} w_{ij} \delta_{r_i, r} \delta_{r_j, r'} \quad (15)$$

denoting the number of edges going from nodes of rank r to nodes of rank r' (i.e. the number of times nodes of

rank r beat nodes of rank r'). By minimizing Eq. 14, we can determine the optimal ranks $\hat{\mathbf{r}}$ and the corresponding optimal strengths $\hat{\boldsymbol{\sigma}} = \{\hat{\sigma}_{\hat{r}_i}\}_{i=1}^N$ that best fit the observed data.

We can see that the first term in Eq. 14 is a constant independent of the underlying node ranking and the second and third terms in Eq. 14 will tend to penalise having a large number of rankings as they will increase $\mathcal{L}(\mathbf{r}, \boldsymbol{\sigma})$. The final two terms are harder to interpret, as they will depend on the particular realisation of the matches. However, empirically, we observe that the fourth term will also penalise having a large number of rankings, while the last term will tend to favour them.

An advantage of working with a Bayesian framework is that it provides us with a principled way to compare results obtained by different models. Suppose we have two different ranking models, which we call \mathcal{H}_1 and \mathcal{H}_2 , that correspond to two different hypotheses for the generating mechanism that produced some observed network of outcomes \mathbf{W} . Let \mathbf{r}_1 and \mathbf{r}_2 be the corresponding most likely rankings obtained by maximising their respective posterior distributions. A principled approach to decide which of the two rankings/model combinations better represents the data is to compute the posterior odds ratio [23]

$$\frac{P(\mathbf{r}_1, \mathcal{H}_1 | \mathbf{W})}{P(\mathbf{r}_2, \mathcal{H}_2 | \mathbf{W})} = \frac{P(\mathbf{W} | \mathbf{r}_1, \mathcal{H}_1) P(\mathbf{r}_1 | \mathcal{H}_1) P(\mathcal{H}_1)}{P(\mathbf{W} | \mathbf{r}_2, \mathcal{H}_2) P(\mathbf{r}_2 | \mathcal{H}_2) P(\mathcal{H}_2)}, \quad (16)$$

where a ratio above (below) 1 indicates that we should favour model \mathcal{H}_1 (\mathcal{H}_2) based on posterior probability. If we assume that the two models are a priori equally likely ahead of observing any data so that $P(\mathcal{H}_1) = P(\mathcal{H}_2)$, we have that the posterior odds ratio can be written as

$$\frac{P(\mathbf{r}_1, \mathcal{H}_1 | \mathbf{W})}{P(\mathbf{r}_2, \mathcal{H}_2 | \mathbf{W})} = \frac{P(\mathbf{W} | \mathbf{r}_1, \mathcal{H}_1) P(\mathbf{r}_1 | \mathcal{H}_1)}{P(\mathbf{W} | \mathbf{r}_2, \mathcal{H}_2) P(\mathbf{r}_2 | \mathcal{H}_2)}. \quad (17)$$

By taking the logarithm of Eq. 17, we can rewrite the posterior odds ratio as

$$\begin{aligned} \log \frac{P(\mathbf{r}_1, \mathcal{H}_1 | \mathbf{W})}{P(\mathbf{r}_2, \mathcal{H}_2 | \mathbf{W})} &= \log P(\mathbf{r}_1, \mathcal{H}_1 | \mathbf{W}) - \log P(\mathbf{r}_2, \mathcal{H}_2 | \mathbf{W}) \\ &= \mathcal{L}_2(\mathbf{r}_2, \mathcal{H}_2) - \mathcal{L}_1(\mathbf{r}_1, \mathcal{H}_1). \end{aligned} \quad (18)$$

C. Optimization

We propose a fast nonparametric agglomerative algorithm based on an alternating optimisation strategy to approximate the MAP estimates $\hat{\mathbf{r}}$, $\hat{\boldsymbol{\sigma}}$ for the node rankings and strengths. Taking the gradient to optimize \mathcal{L} with respect to $\boldsymbol{\sigma}$, while keeping the rank vector \mathbf{r} fixed, yields

$$\sigma_r = \frac{1 + \sum_{r' \neq r} \omega_{rr'} \sigma_{r'} / (\sigma_r + \sigma_{r'})}{2 / (\sigma_r + 1) + \sum_{r' \neq r} \omega_{r'r} / (\sigma_r + \sigma_{r'})} \quad (19)$$

Eq. 19 defines a set of R self-consistent equations for the σ_r 's which can be iteratively solved until convergence.

If $E(\mathbf{r})$ is the number of non-zero entries in the matrix $\boldsymbol{\omega}$ when the ranks are equal to \mathbf{r} , then the complexity of this algorithm is $O(E(\mathbf{r}))$. These iterative updates for the player's strengths have been previously studied in [20], where it was shown that they are guaranteed to converge and do so quite efficiently in practice.

To update \mathbf{r} given $\boldsymbol{\sigma}$, we can greedily identify the pair of consecutive ranks $r < r'$ that produces the largest decrease $\Delta \mathcal{L}(r, r')$ in the negative log-posterior when the two ranks are merged. Let R represent the current number of ranks, and let \mathbf{n} denote the sizes of the rank groups before the merge. The change in the negative log-posterior resulting from merging r and r' is given by:

$$\begin{aligned} \Delta \mathcal{L}(r, r') &= C(R-1) - C(R) + g((r, r')) - g(r) - g(r') \\ &+ f((r, r'), (r, r')) - f(r, r) - f(r', r') - f(r, r') - f(r', r) \\ &+ \sum_{r'' \neq r, r'} [f((r, r'), r'') + f(r'', (r, r')) - f(r, r'') - f(r', r'') \\ &\quad - f(r'', r) - f(r'', r')], \end{aligned} \quad (20)$$

where (r, r') represents the new rank group formed by merging groups r, r' and

$$C(R) = \log N + \log \binom{N-1}{R-1} + \log N!, \quad (21)$$

$$g(r) = - \sum_r \log n_r! + \sum_r \log \left[\frac{(\sigma_r + 1)^2}{\sigma_r} \right], \quad (22)$$

$$f(r, r') = \sum_{r, r'} \omega_{r, r'} \log \left[\frac{\sigma_r + \sigma_{r'}}{\sigma_r} \right]. \quad (23)$$

$C(R)$ accounts for the contribution to the negative log-posterior given by the number of rankings R , $g(r)$ describes contributions from group sizes and strengths, and $f(r, r')$ captures the interaction terms between the rank groups based on the comparison matrix $\boldsymbol{\omega}$ among the rank groups.

Once the ranks to merge have been identified, the optimal strength $\sigma_{(r, r')}$ for the newly merged rank can be determined by solving the following equation:

$$\frac{\partial \Delta \mathcal{L}(r, r')}{\partial \sigma_{(r, r')}} = 0, \quad (24)$$

which leads to

$$\sigma_{(r, r')} = \frac{1 + \sum_{r'' \neq r, r'} \omega_{(r, r') r''} \sigma_{r''} / (\sigma_{(r, r')} + \sigma_{r''})}{2 / (\sigma_{(r, r')} + 1) + \sum_{r'' \neq r, r'} \omega_{r'' (r, r')} / (\sigma_{(r, r')} + \sigma_{r''})}, \quad (25)$$

which is the standard iterative update of Eq. 19 and can be solved efficiently with a computational complexity of $O(E(\mathbf{r})/R)$, where $E(\mathbf{r})$ is now the number of non-zero entries in the matrix $\boldsymbol{\omega}$ for the current ranks \mathbf{r} . When applied across all $R-1$ possible adjacent rank pairs (r, r') , the total complexity for this update and merge process is then $O(E(\mathbf{r}))$.

Having computed the strength for the merged cluster (r, r') , we can repeat the process and do another full update for the strengths σ given the new ranking r after the merge. Again, this requires using the previous iterative update with complexity $O(E(r))$. We can then continue alternating the updates $\sigma|r$ and $r|\sigma$ until all groups have been merged, at which point we can inspect all the examined rankings and select the ranking \hat{r} associated with the highest posterior probability (the lowest value of $\mathcal{L}(r, \sigma)$).

The overall complexity of this algorithm is given by:

$$O\left(\sum_{R=N}^2 E(r)\right) = O(N^{2+\alpha}), \quad (26)$$

where N is the number of nodes or players in the network, r is the optimal rank vector for each value R of the number of unique ranks during the merge process, and $\alpha \in [0, 1]$ depends on the density of the matrix ω as the ranks are progressively merged. In the worst-case scenario, where the matrix ω is maximally dense ($E(r) = R^2$ at every step), the complexity would scale as $O(N^3)$. However, such maximal density is highly unlikely for $R \approx N$, especially in real, sparse networks. In practice, we observe a runtime scaling of approximately $O(N^2)$ with the network size N ; see Fig. 6 in Appendix A. We note that this algorithm is greedy in nature, and therefore is only guaranteed to identify a local optimum for the MAP estimates \hat{r} , $\hat{\sigma}$. However, exact optimization over node groupings is likely NP-hard (as is the case with many other clustering problems [24]), making exact inference intractable in all but the smallest of networks. Greedy agglomerative algorithms have been shown to closely approximate the optimal log posterior probabilities obtained through exact enumeration and simulated annealing for other network clustering tasks in which we expect to preserve spatial contiguity [25, 26] or an initial temporal ordering [27], similar in nature to preserving the initial ordering of the BT scores under the final inferred partial rankings, which is overwhelmingly the case in practice.

Fig. 1 shows the results of applying both the Bradley-Terry (BT) model and our partial rankings model (with the Bradley-Terry likelihood of Eq. 3) to a small dataset of dominance interactions in a pack of wolves [28]. We notice that our model offers a more concise interpretation of the data by grouping individuals with similar BT scores into the same rankings.

Code implementing our partial ranking method can be found in an updated release of the PANINIPy package for nonparametric network inference [29] and at <https://github.com/seb310/partial-rankings>.

III. RESULTS

A. Synthetic Match Datasets

We begin our analysis by evaluating the performance of our algorithm in recovering partial rankings from synthetic data. Specifically, we examine two key sources of uncertainty in ranking recovery: the number of matches played and the separation in player strengths. To achieve this, we design a synthetic model with two tunable parameters, M and σ , which control the number of matches played and the strength separation between players, respectively. The model requires a set of N players and generates matches as follows:

1. For a given value of σ , assign three scores $[-\sigma, 0, \sigma]$ (representing player strengths $[e^{-\sigma}, 1, e^{\sigma}]$) to define the planted partial rankings.
2. Randomly assign each of the N players to one of the three rankings, ensuring that each rank includes at least one player.
3. For a chosen number of matches M , randomly select pairs of players (with repetition) and simulate match outcomes using the Bradley-Terry model.

By varying M and σ , we generate networks of matches with different levels of sparsity and strength separation, allowing us to assess the performance of our algorithm across a wide range of scenarios. Results, shown in Fig. 2, depict the algorithm's ability to recover the planted rankings as a function of σ and the average degree of the network $\langle k \rangle = M/N$. For each $(\sigma, \langle k \rangle)$ pair, 20 different networks were generated, and the results were then averaged.

As expected, we observe that for low values of $\langle k \rangle$, there is not enough evidence to recover the planted rankings regardless of the strength separation between players. In such sparse conditions, the algorithm assigns all players to the same rank, as shown in Fig. 2(a). This behaviour contrasts sharply with the Bradley-Terry (BT) model, which still produces a complete ranking of the nodes even in these highly sparse conditions. As the number of matches increases and the networks become denser, the model gains sufficient statistical evidence to distinguish between the rankings and eventually recovers the planted structure. Notably, the number of matches required to correctly recover the rankings decreases rapidly with greater strength separation between players. In these cases, stronger players consistently outperform weaker ones, creating clearer signals that enable the ranking structure to be resolved with less data.

Perhaps more notable is the fact that our model does not consistently outperform the Bradley-Terry model in scenarios where players are nearly equal in strength. When the separation in player strengths is small, our partial rankings model outperforms BT in sparse networks, as shown in Figs. 2(b)-(c). In these cases, the

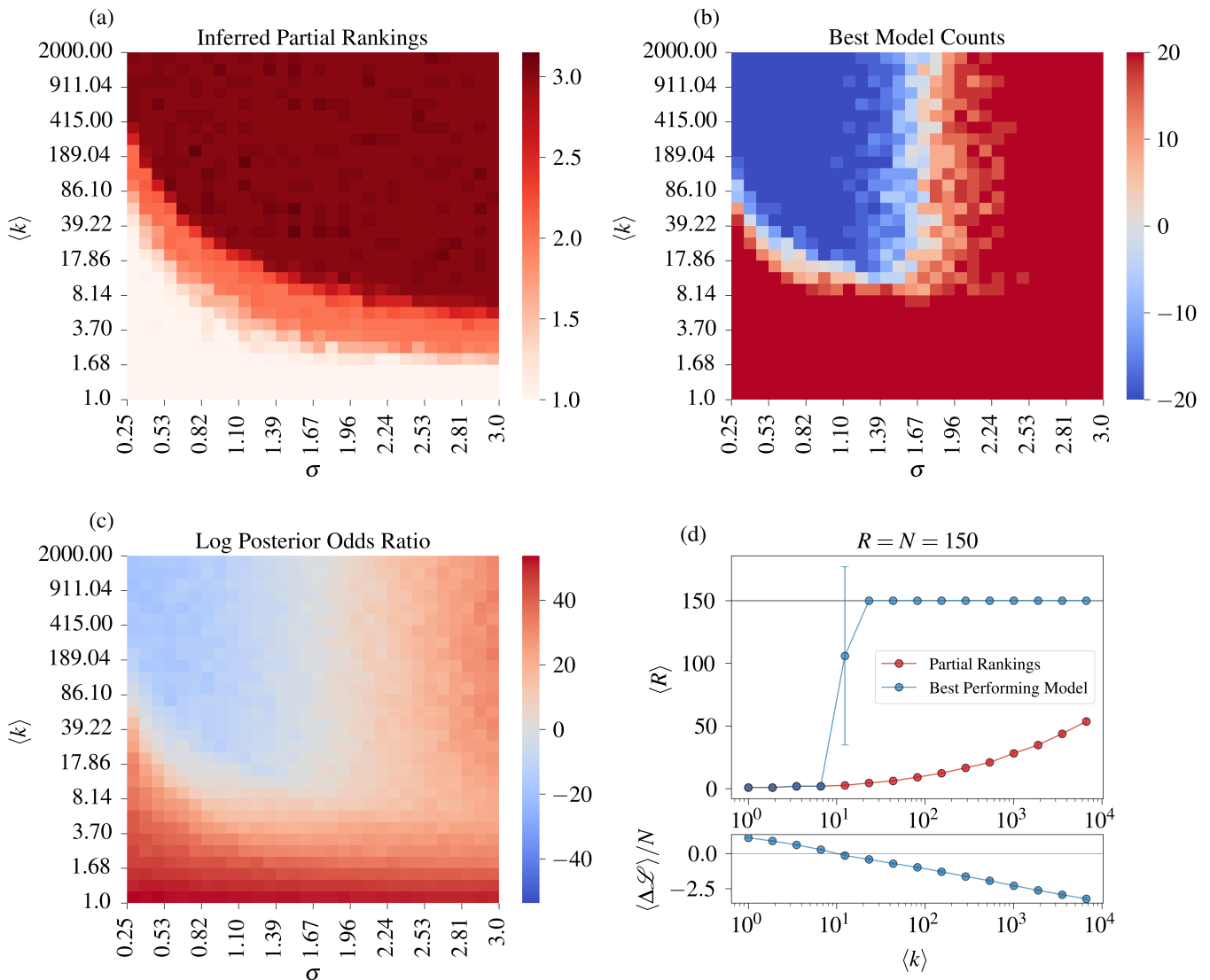


FIG. 2. **Partial rankings in synthetic datasets.** (a) Heatmap of the number of rankings R inferred by the partial rankings model, as a function of the parameters $(\sigma, \langle k \rangle)$ of the synthetic model in Sec. III A. (b) Heatmap of the difference in the total number of times the partial rankings and Bradley-Terry models emerged as the best-performing model (in terms of the posterior odds ratio Eq. 27), out of 20 trials of synthetically generated networks. Positive values indicate that the partial rankings model more often emerged as the best performer, and negative values indicate that the Bradley-Terry model was more often preferred. (c) Heatmap of the log posterior odds ratio (Eq. 27) between the Bradley-Terry and the partial rankings model across the simulations. Positive values indicate a preference for the partial rankings model, and negative values a preference for the Bradley-Terry model. (d) The top panel displays the average number of rankings inferred by the best-performing model (blue) and our partial rankings model (red) as a function of the average degree $\langle k \rangle$ of the network of matches for the case in which no planted partial rankings are present. The bottom panel displays the log posterior odds ratio (normalized per node) between the two models. Negative values of this difference indicate a preference for the Bradley-Terry model and positive values a preference for the partial rankings model. All results were obtained by averaging over 20 different simulations from the synthetic network model of Sec. III A, and error bars indicate 2 standard errors in the mean.

PR model effectively leverages its ability to group players into shared ranks, avoiding overfitting. However, as the networks become denser, while our model accurately recovers the planted rankings even in this low-separation regime, it does not offer a more parsimonious description of the data (in terms of the posterior odds ratio of Eq. 27) compared to the standard Bradley-Terry model which, in

contrast, infers a fully ranked structure for the nodes with $R = N = 50$. This suggests a noisy regime where the evidence supporting partial rankings is relatively weak. The Bradley-Terry likelihood provides a more flexible fit for fine-grained variations in the data in these dense regimes (effectively overfitting the data), even if its prior poorly reflects the underlying data.

In Fig. 2(d), we examine the behaviour of both models in a scenario where no partial rankings are present, and the networks consist of $N = 150$ players, each with its own unique score. The results, averaged over 20 network realisations, show that for small values of $\langle k \rangle$, our partial rankings model still provides a more parsimonious description of the data. However, as $\langle k \rangle$ increases, we observe a sharp transition where the BT model rapidly provides a better description of the data. We also observe that, as $\langle k \rangle$ grows, the PR model gradually infers more rankings, albeit extremely slowly, suggesting that, in principle, the PR model can recover the full ranking given enough data. Interestingly, as the inferred number of groups increases with $\langle k \rangle$, the log posterior odds ratio, defined as

$$\Delta\mathcal{L} = \log \frac{P_{BT}(\boldsymbol{\pi}|\mathbf{A})}{P_{PR}(\boldsymbol{\pi}|\mathbf{A})}, \quad (27)$$

decreases. This is somewhat counterintuitive, as one might expect the posterior odds ratio to improve as the number of rankings inferred by the PR model approaches the true number of rankings. However, as mentioned in Sec. II, the PR model tends to heavily penalise the presence of a large number of rankings so that the net effect of increasing the number of rankings is a reduction in the posterior odds ratio, with the PR model becoming a less efficient encoding for the rankings as the number of inferred groups grows. In practice, the best practice is to evaluate both an original ranking method and our corresponding partial ranking method to determine which provides a more parsimonious fit to the data in terms of log-posterior odds.

To assess the goodness of the recovered partitions, we compute the Kendall rank correlation coefficient (τ_B), adjusted for ties, between the ground truth rankings and the rankings inferred by the BT and PR models. This comparison is performed both when partial rankings are present and when they are not. We observe that when partial rankings are present in the network, the PR model can quickly attain perfect recovery as the networks become denser. On the other hand, while the BT model still achieves high τ_B scores, it never achieves perfect ordinal association and always underperforms relative to the PR model. However, when no partial rankings are present, and each player is assigned a unique score, the roles are reversed, and BT always displays a higher ordinal association with the ground truth rankings (see Appendix B).

We also compare our model with the partial rankings derived by applying 1D mean shift (MS) clustering [30] to the rankings inferred by the BT model. We observe that our algorithm can always recover the correct number of partial rankings when these are present, while MS fails to do so. More importantly, our algorithm can adjust the number of inferred clusters as more data becomes available, even in cases when no partial rankings exist, resulting in a more accurate description of the rankings. In contrast, mean shift clustering consistently infers roughly the same number of partial rankings regardless of the ev-

idence provided by the data (see Appendix C).

B. Real Match Datasets

In this section we focus on how our partial rankings algorithm may be used to derive meaningful patterns in real-world data. We consider the datasets compiled in [6] and available at [48]. In addition, we also consider a dataset of social hierarchies among a pack of wolves [20, 28], and other sets of directed networks available at [49]. The datasets are summarized in Table I.

We apply our partial rankings algorithm and the Bradley-Terry model to all match lists in the dataset and compare the results. In Fig. 3(a), we show the number of inferred ranks per node and the value of the log posterior odds ratio per node as a function of the average degree of each network. To standardise the number of ranks per node within the interval $[0, 1]$, we rescale it as $(R - 1)/(N - 1)$, where N is the number of nodes in the network and R is the total number of ranks inferred by the best-performing model. This quantity will be 1 for perfect orderings in which $R = N$. It will be 0 if no rankings are inferred and all nodes are assigned the same strength, and it will take intermediate values when non-trivial partial rankings are present. The data reveals three distinct phases based on the density of the underlying network. For low average degree values, $\langle k \rangle$, the evidence is insufficient to support any meaningful ranking, leading to all actors being assigned the same strength. As connectivity increases, partial rankings begin to offer a more parsimonious description of the data compared to a perfect ordering of the nodes. In this intermediate regime, non-trivial subdivisions emerge, where actors are grouped by strength: all nodes within a group share the same strength, but strengths vary across groups. Finally, as the networks become sufficiently dense, enough data is available to support a perfect ordering of the nodes, and the Bradley-Terry model provides a more parsimonious description of the data.

To evaluate the homogeneity in the distribution of rank sizes, we adapt the concept of the *effective number of groups* from the community detection literature [50] and define the *effective number of rankings*. If R is the number of rankings inferred by the PR algorithm, we can express the effective number of rankings R^* as

$$R^* = \exp \left(- \sum_{r=1}^R \frac{n_r}{N} \log \frac{n_r}{N} \right), \quad (28)$$

where n_r is the size of rank r and N is the total number of nodes in the network. This measure reflects the balance in the size distribution of rankings: R^* will achieve a maximum value of R when all the rankings are of equal size. In contrast, it approaches a minimal value close to one when the distribution is highly imbalanced, with most nodes concentrated in a single

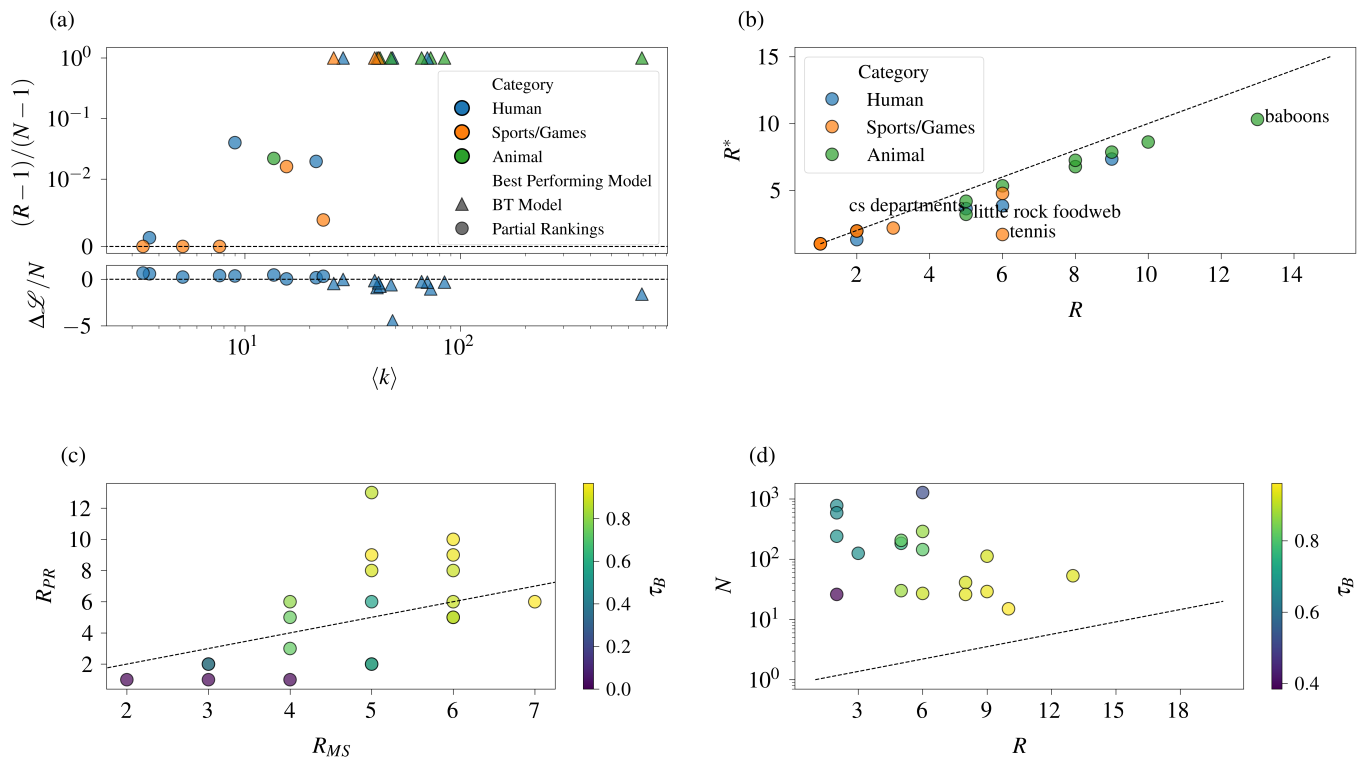


FIG. 3. **Partial rankings in real networks of pairwise comparisons.** (a) (top) Rescaled number of ranks per node inferred by the best-performing model and (bottom) log posterior odds ratio per node, both as a function of the average degree for all real-world networks considered in the study (see Table 1). The colours of the points indicate the different categories to which the datasets belong, while the shape of the markers indicates which model (PR or BT) emerged as the best-performing method (in terms of the posterior odds ratio). Positive values of the log posterior odds ratio indicate evidence in favour of the PR model; negative values indicate evidence in favour of the BT model. (b) Effective number of ranks, R^* (Eq. 28), as a function of the number of unique ranks R inferred by the PR algorithm. The black dashed line represents the line $R^* = R$. (c) Number of rankings inferred via the partial rankings algorithm as a function of the number of rankings inferred via mean shift clustering. Point colours indicate the τ_B score between the two inferred rankings. The black dashed line represents the line $R_{PR} = R_{MS}$. (d) Number of nodes of each network as a function of the number of rankings R inferred by the partial rankings algorithm. Point colours indicate the τ_B score between the rankings inferred via the partial rankings algorithm and those inferred by the Bradley-Terry model. The dashed black line indicates the line $R = N$.

rank. Fig. 3(b) shows the R^* as a function of the inferred partial rankings R for the PR model. While for most datasets $R^* \simeq R$, indicating that in most cases the PR algorithm infers roughly equally sized rankings, there are some notable exceptions, most notably the dataset of ATP tennis matches between 2010 and 2019, which displays a considerably smaller effective number of groups, reflecting a pronounced imbalance in the sizes of the inferred ranks. Specifically, the strongest 15 players are distributed across three partial rankings, while over 84% of all players are grouped into the weakest rank. This skewed decomposition likely stems from the structure of professional tennis tournaments. ATP matches are generally organised in a knock-out format, where losers are progressively eliminated. While this structure is efficient and straightforward, it can result in noisy rankings, as strong players may be eliminated early due to random fluctuations or unfavourable matchups. To mitigate this, the ATP organises multiple knock-out tournaments

throughout the year, ensuring that the strongest players consistently rise to the top despite potential variability in individual tournaments. However, this system disproportionately concentrates matches among the strongest players, who predominantly compete against one another as they progress through the brackets. Consequently, the dataset contains ample information to distinguish the strongest players but far less data to differentiate among weaker players, leading to highly unbalanced partial rankings in terms of size.

Again, we compare the results obtained via our PR algorithm with those obtained by applying 1D Mean Shift clustering to the rankings inferred by the Bradley-Terry model. In Fig. 3(c), we plot the number of partial rankings, R_{PR} , inferred by the PR algorithm against the number of partial rankings, R_{MS} , inferred by Mean Shift. While a general positive correlation is observed between the two quantities, there is significant variability in the number of rankings inferred by the two methods. More-

Data set	N	M	$\langle k \rangle$	R	R^*	$\Delta\mathcal{L}$	Category	Description	Ref.
Soccer	2204	7438	3.4	1	1	1469.3	Sports/games	Men’s international association football matches 2010 - 2019	[31]
Friends	774	2799	3.6	2	2.0	450.1	Human	High-school friend nominations	[32]
Tennis	1272	29397	23.1	6	1.7	404.9	Sports/games	Association of Tennis Professionals matches 2010–2019	[33]
Chess	917	7007	7.6	1	1	357.5	Sports/games	Online chess games on lichess.com in 2016	[34]
Little Rock food web	183	2494	13.6	5	3.2	83.7	Animal	Food web among the species in Little Rock Lake in Wisconsin	[35]
CS departments	205	34388	21.4	5	3.6	33.4	Human	PhD graduates of one department hired as faculty in another	[18]
College football	115	593	5.2	1	1	26.8	Sports/games	NCAA College Football matches 2013-2023	[36]
Dutch school friends	26	234	9.0	2	1.3	9.2	Human	Friendships at secondary school in The Netherlands, 2003-2004	[37]
Video games	125	1951	15.6	3	2.2	4.7	Sports/games	<i>Super Smash Bros Melee</i> tournament matches in 2022	[38]
History departments	144	4112	28.6	6	3.8	-3.2	Human	PhD graduates of one department hired as faculty in another	[18]
Hyenas	29	1913	66.0	9	7.9	-7.6	Animal	Dominance interactions among hyenas in captivity	[39]
Sparrows	26	1238	47.6	8	7.3	-15.4	Animal	Attacks and avoidances among sparrows in captivity	[40]
Baboons	53	4464	84.2	13	10.3	-16.3	Animal	Dominance interactions among baboons in captivity	[41]
Dogs	27	1143	42.3	6	5.3	-20.3	Animal	Aggressive behaviors in a group of domestic dogs	[42]
Wolf	15	10382	692.1	10	8.6	-24.0	Animal	Dominance interaction among wolves in captivity	[28]
Mice	30	1230	41.0	5	4.2	-26.8	Animal	Dominance interactions among mice in captivity	[43]
Business departments	112	7856	70.1	9	7.3	-35.2	Human	PhD graduates of one department hired as faculty in another	[18]
Vervet monkeys	41	2980	72.7	8	6.8	-42.7	Animal	Dominance interactions among a group of wild vervet monkeys	[44]
Scrabble	587	23477	40.0	2	2.0	-86.0	Sports/games	<i>Scrabble</i> tournament matches 2004–2008	[45]
Basketball	240	10002	41.7	2	2.0	-90.7	Sports/games	National Basketball Association games 2015–2022	[46]
Soccer (aggregated)	288	7438	25.8	6	4.8	-131.1	Sports/games	Soccer dataset above aggregated across 2010 - 2019	[31]
UN migrations	232	11228	48.4	194	183.2	-1036.5	Human	Migrations between countries 1990 - 2015	[47]

TABLE I. Datasets analysed using the partial rankings algorithm and Bradley-Terry algorithm, in order of decreasing log posterior odds ratio in Eq. 27 (i.e. increasingly in favor of the original Bradley-Terry model). N , M , and $\langle k \rangle$ indicate the number of nodes, edges, and average degree of each network, respectively. R and R^* indicate the number of partial rankings inferred via the PR algorithm and the effective number of partial rankings (Eq. 28). \mathcal{L} indicates the logarithm of the posterior odds ratio between the PR and BT models (Eq. 27).

over, even when the total number of rankings inferred by both algorithms is similar, the rankings themselves may differ substantially, as evidenced by the Kendall rank correlation (τ_B) scores also shown in Fig. 3(c). Specifically, τ_B scores appear to increase with the total number of groups inferred by both algorithms, regardless of how close R_{PR} and R_{MS} are. This suggests that the increase in τ_B scores is likely an artefact resulting from the fact that the algorithms are likely to align on most pairwise relationships as the number of groups grows rather than reflecting a similarity in the group structures inferred by the two approaches.

Finally, we also compare the results inferred by our algorithm with those obtained by the BT model. Fig. 3(d) shows the number of nodes N in each network as a function of the rankings R inferred by the partial rankings algorithm, where the points are coloured according to the τ_B score between the rankings inferred by the PR and BT models. Again, we observe a general tendency for the τ_B scores to increase as R approaches N .

C. Case Study: CS Faculty Hiring

As a case study, we apply our algorithm to a dataset of faculty hires in Computer Science (CS) departments at U.S. higher education institutions, compiled in [18] for analysis of hierarchies in faculty hiring using a different ranking methodology. Each node represents one of the

205 PhD-granting institutions included in the study and a directed edge (i, j) exists from institution i to institution j for each individual who earned their doctorate at i and held a tenure or tenure-track faculty position at j during the collection period from May 2011 to March 2012. For 153 of these institutions, their *U.S. News & World Report* rankings (USN rankings) are available in the form of node metadata, which we use to compare against the rankings and partial rankings inferred by the two pairwise ranking methods employed in this study. Additionally, we manually collected endowment data for 151 of the 153 institutions with associated USN rankings.

Fig. 4(a) shows the results of applying the Bradley-Terry model and our partial rankings algorithm to the entire set of 205 PhD granting institutions. Each bar represents an institution, ordered by its BT rank, with bar heights representing the BT strength scores. Bars are colour-coded according to their PR rankings, with corresponding strengths shown in the legend in Fig. 4(b). The rankings are dominated by a small group of elite universities displaying significantly higher strengths, followed by a sharp decline in strength values further down the list. The PR and BT rankings show strong ordinal association ($\tau_B = 0.82$; p-value = 1.2×10^{-53}) with only a small number of rank violations—instances where $\text{rank}_{BT}(A) > \text{rank}_{BT}(B)$ but $\text{rank}_{PR}(A) < \text{rank}_{PR}(B)$ —at the boundary between the two lowest-scoring PR groups, possibly indicating a lack of information to accurately determine the group boundaries.

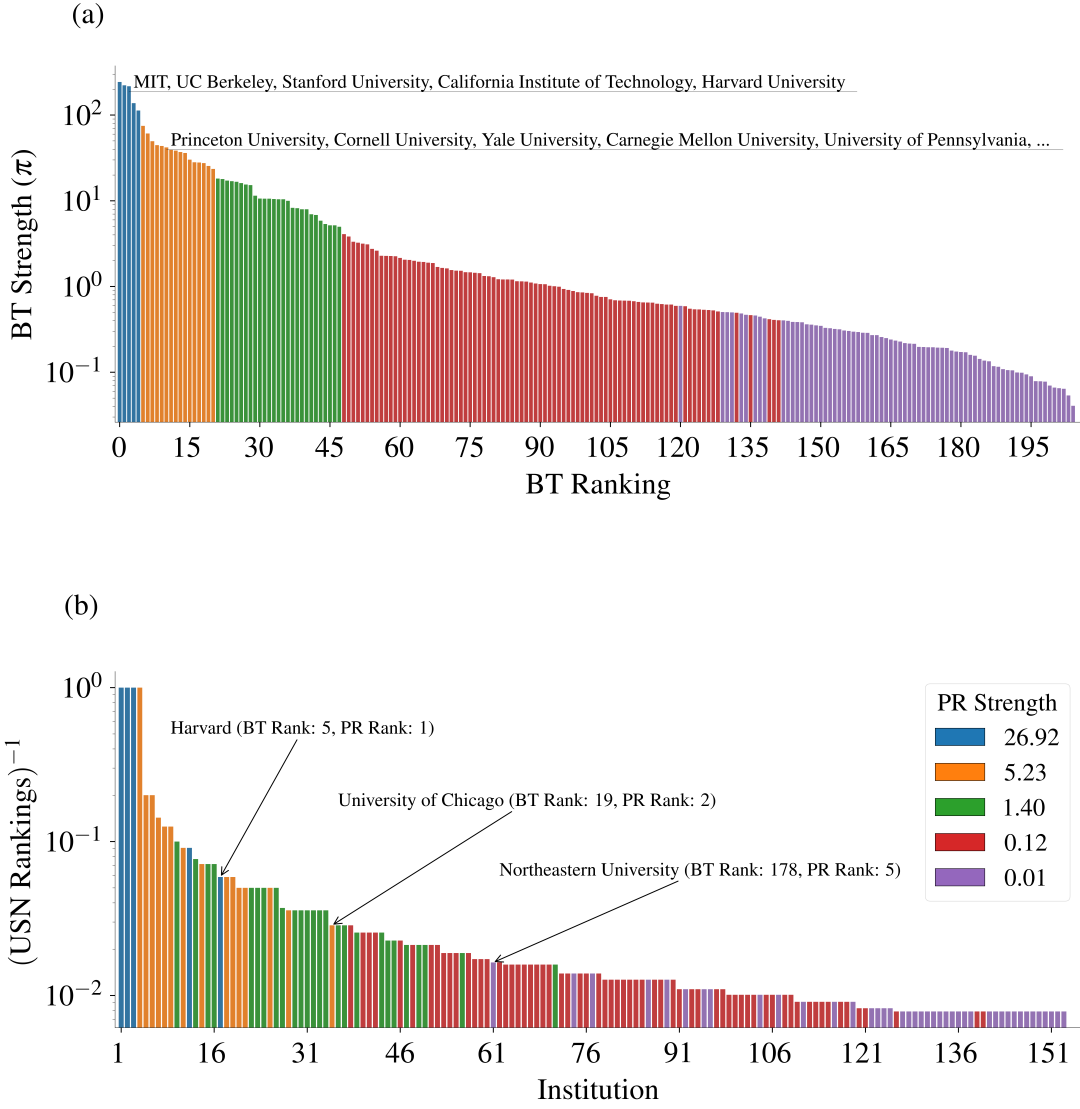


FIG. 4. **Partial rankings of CS departments according to faculty hiring patterns.** (a) Barplot of BT strengths for the 205 PhD granting institutions included in the dataset, ordered according to their inferred BT rankings. Colours indicate the PR membership of each institution. A legend displaying the numerical values of these PR strengths is shown in panel (b). The names of the five institutions making up the strongest PR cluster and of the first five institutions in the second-strongest PR cluster (ordered in terms of their BT rank) are shown in the figure. (b) Barplot depicting the inverse of the USN ranking score for the 153 institutions for which data was available. Colours indicate the corresponding PR membership of each institution. Some notable inconsistencies between the USN rankings of some institutions and those inferred by pairwise comparison methods are shown in the figure.

In Fig. 4(b), we compare the partial rankings inferred by our model with the *U.S. News & World Report* rankings. Each bar in the plot represents a PhD-granting institution, ordered by its USN rank, with bar heights corresponding to the inverse of their USN rank. Again, bars are colour-coded according to their partial rankings inferred by the PR model.

One first thing to notice with regards to the USN rankings is that they allow for partial rankings. For example, the four highest-scoring universities according to the USN methodology are all assigned an equal rank of 1. Fig. 4(b) reveals that institutions with equal USN rank-

ing often belong to the same partial rankings according to the PR model. However, the PR model generally produces broader rankings, grouping institutions that span a wider range of USN ranks. Another striking feature is the significantly higher number of rank violations, although the overall ordinal association remains strong ($\tau_B = 0.76$; p-value = 1.37×10^{-33}). Some of these rank violations are particularly striking. For example, Harvard University, ranked 5th in the BT model and belonging to the top-scoring PR group, is ranked 17th according to the USN rankings, behind institutions including the University of Maryland, College Park (26th in the BT model and in the

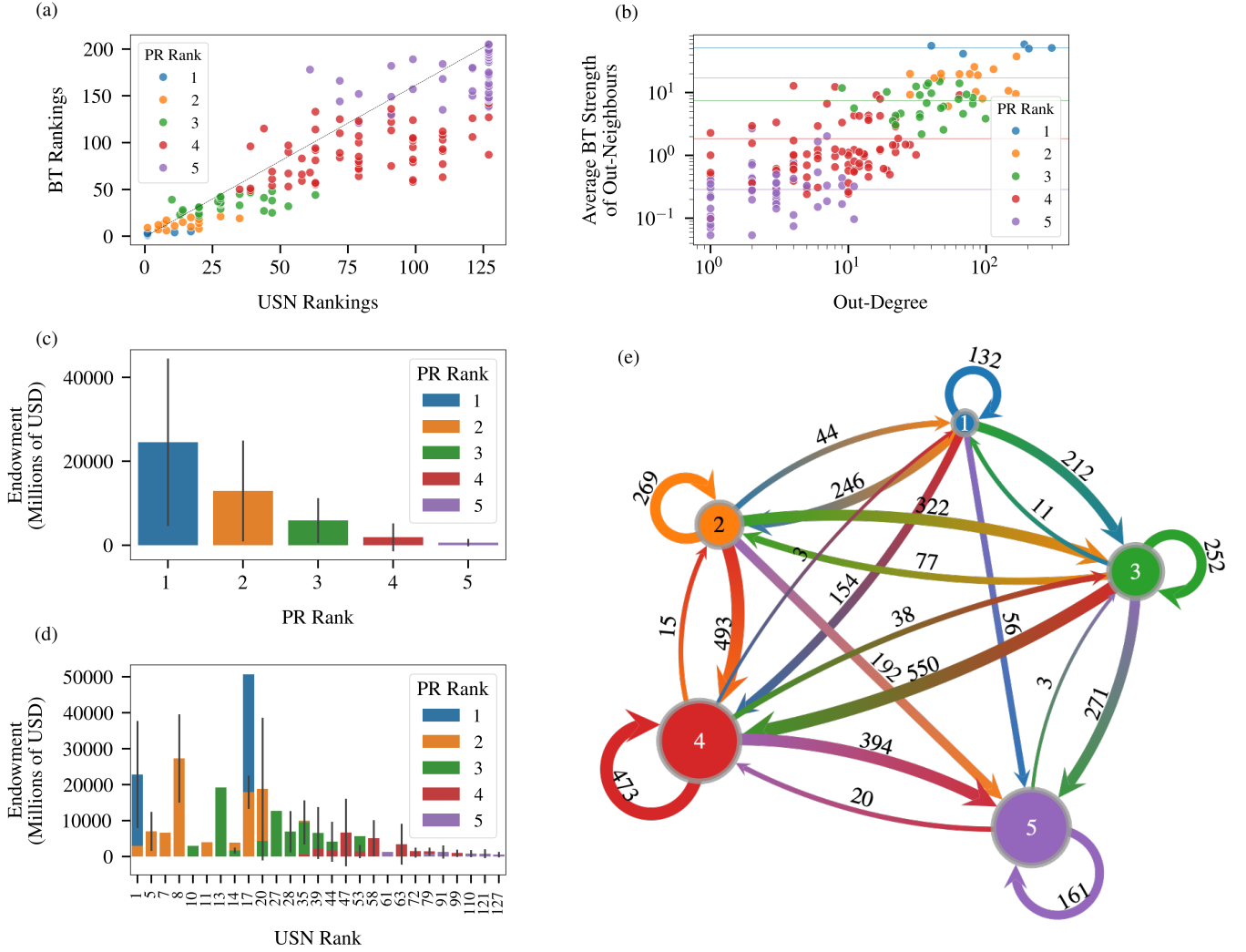


FIG. 5. **Partial rankings of CS departments and their external metadata.** (a) BT rankings as a function of USN rankings for all 153 PhD granting institutions that had associated USN ranking. Points are coloured according to their PR rank. The black dashed line corresponds to the case $R_{BT} = R_{USN}$. (b) Average BT strength of a node’s out-neighbours as a function of the node’s out-degree. Points are coloured according to their PR rank. The horizontal lines represent the average BT score of the out-neighbours disaggregated by PR group. (c) Average endowment (in millions of USD) for the institutions in each partial rank. Error bars represent the standard deviations within each partial rank group. (d) Average endowment (in millions of USD) as a function of the USN rank, disaggregated by partial rankings. Error bars represent the standard deviations within each group of universities binned by USN rank (including ties). (e) Network representation of faculty hiring flows among the partial rank groups inferred by our algorithm. Each node represents a partial ranking, with labels and colours indicating the corresponding group. Node sizes are proportional to the number of institutions assigned to each partial ranking. Directed edges represent the hiring flows between groups, with edge thickness proportional to the net flow. Edge colours transition from the origin node’s colour at the base to the destination node’s colour at the arrowhead and the net flow value is annotated on each edge.

third PR group) that scored significantly lower according to the hiring network structure. Similarly, the University of Chicago is ranked 19th by the BT model and belongs to the second highest-scoring PR group but is ranked 35th in the USN rankings. While the *U.S. News & World Report* utilises a wide array of metrics to conduct its rankings, such as peer assessment scores, graduation and retention rates, and financial resources, this result would appear to suggest that these factors may not directly align with

academic job market preferences. In the case of Harvard University or the University of Chicago, one might surmise that the prestigious reputation of the institutions might be influencing the job market more than their USN rankings. The opposite effect can also be observed. For instance, Northeastern University, ranked 61st in the USN rankings, is assigned 178th place by the BT model and belongs to the lowest PR group despite its considerably higher USN ranking. This suggests that perhaps this

program was undervalued in the job market relative to its academic credentials during the period studied.

To evaluate how the BT rankings compare to the USN rankings, Fig. 5(a) plots the BT rank of each institution against its corresponding USN rank, with points colour-coded based on their PR rank. The highest-ranking institutions, according to both models, tend to concentrate around the $R_{BT} = R_{USN}$ line, where R_{BT} and R_{USN} represent the Bradley-Terry and USN rankings respectively—indicating close agreement between the two ranking systems for top-tier institutions. As we move towards lower-ranked institutions, we observe an increasing divergence between the rankings. While the overall ordinal association remains strong ($\tau_B = 0.73$, p-value = 1.07×10^{-38}), the spread in rankings widens, and institutions with a given USN rank are often assigned considerably different BT ranks, with the BT model frequently assigning these institutions higher positions compared to the USN rankings. This discrepancy is particularly pronounced among institutions in the two lowest-scoring PR groups.

An interesting question about the pairwise ranking methods considered in this work is whether an institution’s rank benefits more from “who you win against” than from the sheer number of “wins”. In other words, does an institution’s ranking improve more by producing a large number of doctoral graduates who secure tenure-track positions across a wide range of institutions or by producing fewer graduates who secure positions at highly ranked institutions? To address this, in Fig. 5(b), we plot the average BT strength of an institution’s out-neighbors (capturing the quality of an institution’s “wins”) as a function of its out-degree (representing the total number of “wins” an institution has). We observe a clear positive correlation (Pearson $p = 0.78$; p-value = 1.32×10^{-43}) with the highest ranked institutions having both a large number of “wins” (i.e. producing a large number of graduates that go on to secure tenure-track positions at other institutions), as well as out-neighbours with high BT strengths (i.e. their graduates tend to secure positions at high-ranking institutions). Perhaps more revealing is the fact that the PR groups appear to stratify according to the average BT strength of their out-neighbours, suggesting a well-defined hierarchy characterised by a predominance in horizontal mobility as opposed to vertical mobility. This observation is reinforced by analysing the network of mobility flows between the PR groups; see Fig. 5(e). The results reveal a well-defined hierarchy with minimal upward mobility across ranks. Most mobility occurs downward within the hierarchy, a trend partly explained by the relatively small size of the top-ranked groups. Nonetheless, horizontal mobility emerges as a critical driver of hiring dynamics across all levels, particularly within the lower-ranked groups, where it becomes the dominant hiring pattern. Horizontal mobility is particularly pronounced at the topmost level of the hierarchy, where the top five institutions comprising this elite group hire over twice as many faculty members from

within their group as they do from all other PhD granting institutions combined.

Finally, we note that the ranking patterns possess a moderately strong ordinal association with the endowments of the institutions. Although there is considerable variability, higher-ranked institutions generally tend to have significantly larger endowments, as illustrated in Fig. 5 (c)-(d).

IV. CONCLUSION

We have introduced a probabilistic generative model for inferring partial rankings in directed networks and a fast, fully nonparametric, agglomerative algorithm for efficient inference. We have shown that, particularly with limited observations available, our model can provide a more parsimonious description of pairwise comparison data than models that inherently assume complete rankings such as the BT model. Specifically, in extremely sparse regimes, our model effectively recognises that insufficient evidence exists to infer any meaningful ranking among the compared entities. As the network’s connectivity increases, partial rankings typically emerge as a more compact and accurate description of the data. Finally, as we move towards more dense regimes, we reach a point where sufficient information is available to infer a complete ordinal ranking of all the nodes. When applied to a network of faculty hiring among U.S. computer science departments, our algorithm inferred five distinct partial rankings, which align closely with the ordinal rankings inferred by the BT model and reveal a well-defined hierarchy dominated by a small number of elite universities. The inferred rankings also highlight the limited upward mobility within the hierarchy, with lateral and downward movements being more prevalent.

There are several directions in which our work can be extended. While widely used, the classical Bradley-Terry model represents a relatively simplistic approach to pairwise interactions between entities. Numerous extensions to the model have been proposed, including accounting for ties [12, 13], home-field advantage [11], randomness in match outcomes, and imbalances in strength or skill between the average pair of players [6]. Any of these extensions could, in principle, be incorporated into our partial rankings framework, enabling the development of more expressive models.

Another characteristic of both the Bradley-Terry model and our partial rankings framework is that they do not explicitly account for the placement of edges in the network—that is, the likelihood does not include a term that models the probability of observing a given set of matches in the first place. As we observed in Sec. III C, similarly (partially) ranked institutions tend to interact primarily with one another. A similar observation holds for the ATP tennis dataset, where the strongest players, who advance through the tournament, tend to play more matches and preferentially against each

other. While other methods explicitly model edge placement [9, 10], this aspect remains absent from the current Bradley-Terry and partial rankings models. Incorporating it into the framework could help to explore how network topology influences ranking recovery.

Finally, our framework could be extended to consider other cases of interest, such as dynamic rankings, where the ranks of the individual entities can rise or fall over time [17], personalised rankings, in which ranking results are tailored to individual users based on their prefer-

ences [51], or a combination of both.

ACKNOWLEDGMENTS

The authors acknowledge funding support from the HKU-100 Start Up Fund and an HKU Urban Systems Institute Fellowship Grant, and Max Jerdee for helpful discussions about the datasets.

-
- [1] J. T. Whelan, Prior distributions for the bradley-terry model of paired comparisons. *arXiv preprint arXiv:1712.05311* (2017).
- [2] R. R. Davidson and D. L. Solomon, A bayesian approach to paired comparison experimentation. *Biometrika* **60**(3), 477–487 (1973).
- [3] A. N. Langville and C. D. Meyer, *Who’s# 1? The Science of Rating and Ranking*. Princeton University Press (2012).
- [4] H. A. David, *The Method of Paired Comparisons*, volume 12. London (1963).
- [5] R. A. Bradley and M. E. Terry, Rank analysis of incomplete block designs: I. the method of paired comparisons. *Biometrika* **39**(3/4), 324–345 (1952).
- [6] M. Jerdee and M. Newman, Luck, skill, and depth of competition in games and social hierarchies. *Science Advances* **10**(45), eadn2654 (2024).
- [7] A. E. Elo and S. Sloan, The rating of chessplayers: Past and present. (*No Title*) (1978).
- [8] R. Herbrich, T. Minka, and T. Graepel, Trueskill™: a bayesian skill rating system. *Advances in Neural Information Processing Systems* **19** (2006).
- [9] C. De Bacco, D. B. Larremore, and C. Moore, A physical model for efficient ranking in networks. *Science Advances* **4**(7), eaar8260 (2018).
- [10] T. P. Peixoto, Ordered community detection in directed networks. *Physical Review E* **106**(2), 024305 (2022).
- [11] A. Agresti, *Categorical Data Analysis*, volume 792. John Wiley & Sons (2012).
- [12] P. Rao and L. L. Kupper, Ties in paired-comparison experiments: A generalization of the bradley-terry model. *Journal of the American Statistical Association* **62**(317), 194–204 (1967).
- [13] R. R. Davidson, On extending the bradley-terry model to accommodate ties in paired comparison experiments. *Journal of the American Statistical Association* **65**(329), 317–328 (1970).
- [14] T. Yan, Ranking in the generalized bradley-terry models when the strong connection condition fails. *Communications in Statistics-Theory and Methods* **45**(2), 340–353 (2016).
- [15] R. Baker and P. Scarf, Modifying bradley-terry and other ranking models to allow ties. *IMA Journal of Management Mathematics* **32**(4), 451–463 (2021).
- [16] L. Iacovissi and C. De Bacco, The interplay between ranking and communities in networks. *Scientific Reports* **12**(1), 8992 (2022).
- [17] A. Della Vecchia, K. Neocosmos, D. B. Larremore, C. Moore, and C. De Bacco, Model for efficient dynamical ranking in networks. *Physical Review E* **110**(3), 034310 (2024).
- [18] A. Clauset, S. Arbesman, and D. B. Larremore, Systematic inequality and hierarchy in faculty hiring networks. *Science Advances* **1**(1), e1400005 (2015).
- [19] E. Zermelo, Die berechnung der turnier-ergebnisse als ein maximumproblem der wahrscheinlichkeitsrechnung. *Mathematische Zeitschrift* **29**(1), 436–460 (1929).
- [20] M. Newman, Efficient computation of rankings from pairwise comparisons. *Journal of Machine Learning Research* **24**(238), 1–25 (2023).
- [21] L. R. Ford Jr, Solution of a ranking problem from binary comparisons. *The American Mathematical Monthly* **64**(8P2), 28–33 (1957).
- [22] F. Caron and A. Doucet, Efficient bayesian inference for generalized bradley-terry models. *Journal of Computational and Graphical Statistics* **21**(1), 174–196 (2012).
- [23] E. T. Jaynes, *Probability Theory: The Logic of Science*. Cambridge University Press (2003).
- [24] W. J. Welch, Algorithmic complexity: three np-hard problems in computational statistics. *Journal of Statistical Computation and Simulation* **15**(1), 17–25 (1982).
- [25] A. Kirkley, Spatial regionalization based on optimal information compression. *Communications Physics* **5**(1), 249 (2022).
- [26] S. Morel-Balbi and A. Kirkley, Bayesian regionalization of urban mobility networks. *Physical Review Research* **6**(3), 033307 (2024).
- [27] A. Kirkley, Inference of dynamic hypergraph representations in temporal interaction data. *Physical Review E* **109**(5), 054306 (2024).
- [28] J. A. van Hooff and J. Wensing, 11. dominance and its behavioral measures in a captive wolf pack. *Man Wolf Adv. Issues Probl. Captive Wolf Res* **4**, 219 (1987).
- [29] A. Kirkley and B. He, PANINIPy: Package of algorithms for nonparametric inference with networks in python. *Journal of Open Source Software* **9**(103), 7312 (2024).
- [30] D. Comaniciu and P. Meer, Mean shift: A robust approach toward feature space analysis. *IEEE Transactions on Pattern Analysis and Machine Intelligence* **24**(5), 603–619 (2002).
- [31] M. Jürisoo, International Men’s Football Results from 1872 to 2023. <https://www.kaggle.com/datasets/martj42/international-football-results-from-1872-to-2017>.

- [32] P. S. B. J. R. Udry and K. M. Harris, National Longitudinal Study of Adolescent Health (1997. [NationalLongitudinalStudyofAdolescentHealth\(1997\)](https://www.icpsr.org/studies/sna/nsal/)).
- [33] J. Sackmann, ATP Tennis Data. https://github.com/JeffSackmann/tennis_atp.
- [34] A. Revel, Online Chess Match Data from lichess.com. <https://www.kaggle.com/datasets/arevel/chess-games>.
- [35] N. D. Martinez, Artifacts or attributes? effects of resolution on the little rock lake food web. *Ecological Monographs* **61**(4), 367–392 (1991).
- [36] J. Gallini, College Football Team Stats Seasons 2013 to 2023. <https://www.kaggle.com/datasets/jeffgallini/college-football-team-stats-2019>.
- [37] T. A. Snijders, G. G. Van de Bunt, and C. E. Steglich, Introduction to stochastic actor-based models for network dynamics. *Social Networks* **32**(1), 44–60 (2010).
- [38] Super Smash Bros. Melee Head to Head Records. <https://etossed.github.io/rankings.html>.
- [39] E. D. Strauss and K. E. Holekamp, Social alliances improve rank and fitness in convention-based societies. *Proceedings of the National Academy of Sciences* **116**(18), 8919–8924 (2019).
- [40] D. J. Watt, Relationship of plumage variability, size and sex to social dominance in harris’ sparrows. *Animal Behaviour* **34**, 16–27 (1986).
- [41] M. Franz, E. McLean, J. Tung, J. Altmann, and S. C. Alberts, Self-organizing dominance hierarchies in a wild primate population. *Proceedings of the Royal Society B: Biological Sciences* **282**(1814), 20151512 (2015).
- [42] M. J. Silk, M. A. Cant, S. Cafazzo, E. Natoli, and R. A. McDonald, Elevated aggression is associated with uncertainty in a network of dog dominance interactions. *Proceedings of the Royal Society B* **286**(1906), 20190536 (2019).
- [43] C. M. Williamson, B. Franks, and J. P. Curley, Mouse social network dynamics and community structure are associated with plasticity-related brain gene expression. *Frontiers in Behavioral Neuroscience* **10**, 152 (2016).
- [44] C. Vilette, T. Bonnell, P. Henzi, and L. Barrett, Comparing dominance hierarchy methods using a data-splitting approach with real-world data. *Behavioral Ecology* **31**(6), 1379–1390 (2020).
- [45] Scrabble Tournament Records. <https://www.cross-tables.com/>.
- [46] N. Lauga, NBA Games Data. <https://www.kaggle.com/datasets/nathanlauga/nba-games/data>.
- [47] United Nations Department of Economic and Social Affairs Population Division (2015), “Trends in International Migrant Stock: The 2015 Revision.” (United Nations Database, POP/DB/MIG/Stock/Rev.2015). <https://www.un.org/en/development/desa/population/migration/data/estimates2/estimates15.asp>.
- [48] M. Jerdee, pairwise-ranking. <https://github.com/maxjerdee/pairwise-ranking>.
- [49] T. P. Peixoto, The Netzschleuder Network Catalogue and Repository. <https://networks.skewed.de/>.
- [50] M. A. Riolo, G. T. Cantwell, G. Reinert, and M. E. Newman, Efficient method for estimating the number of communities in a network. *Physical Review E* **96**(3), 032310 (2017).
- [51] S. Rendle, C. Freudenthaler, Z. Gantner, and L. Schmidt-Thieme, BPR: Bayesian personalized ranking from im-

PLICIT feedback. *arXiv preprint arXiv:1205.2618* (2012).

Appendix A: Time Complexity

In Fig. 6, we plot the runtime of our algorithm as a function of the number of nodes N in the network for both synthetically generated data (Fig. 6(a)) and empirical networks (Fig. 6(b)). The results display an approximately quadratic scaling of the runtime with N (see Sec. II), with some variation in the real datasets due to varying densities of edges present.

Appendix B: Tau Recovery

In Fig. 7, we show Kendall’s τ_B rank correlation coefficient as a function of the average degree for synthetically generated networks consisting of $N = 150$ nodes. Panel (a) corresponds to the case $R = N = 150$, where each node is assigned a unique ranking, implying no partial rankings are present. Panel (b) illustrates the scenario where $R = 3$ unique partial rankings are imposed, with the nodes distributed at random among these three ranks.

In the case where no partial rankings are present (panel (a)), we observe that the BT model consistently outperforms the PR model in terms of rank correlation with the ground truth rankings, with the PR model obtaining similar $\langle \tau_B \rangle$ scores only at very high values of $\langle k \rangle$. Note that, as shown in Fig. 2(d), the PR model never recovers the correct number of rankings, even in dense regimes. However, the PR model is able to increase the inferred number of partial rankings as more data becomes available, which improves its rank correlation with the ground truth. By the time the PR model infers approximately $R = 50$ rankings, it achieves τ_B scores of roughly 0.99.

When partial rankings are present (panel (b)), the $\langle \tau_B \rangle$ value for the BT model plateaus around 0.8. This behaviour likely stems from the Bradley-Terry model’s inherent assumption of a complete ranking, which limits its ability to adapt once it has achieved the best possible alignment it can with the ground truth rankings. On the other hand, the PR model is able to obtain perfect correlation already at relatively low values of $\langle k \rangle$, thanks to its ability to account for and adapt to the presence of partial rankings in the data.

Appendix C: Comparison with 1D Clustering

In Fig. 8, we show the number of partial ranks inferred by using our partial rankings algorithm and mean shift clustering [30] for (a) the case in which no partial rankings are present ($R = N = 150$) and (b) the case with $R = 3$ planted partial rankings to which the nodes are assigned. When partial rankings are present (panel (b)), we observe that our partial rankings algorithm is

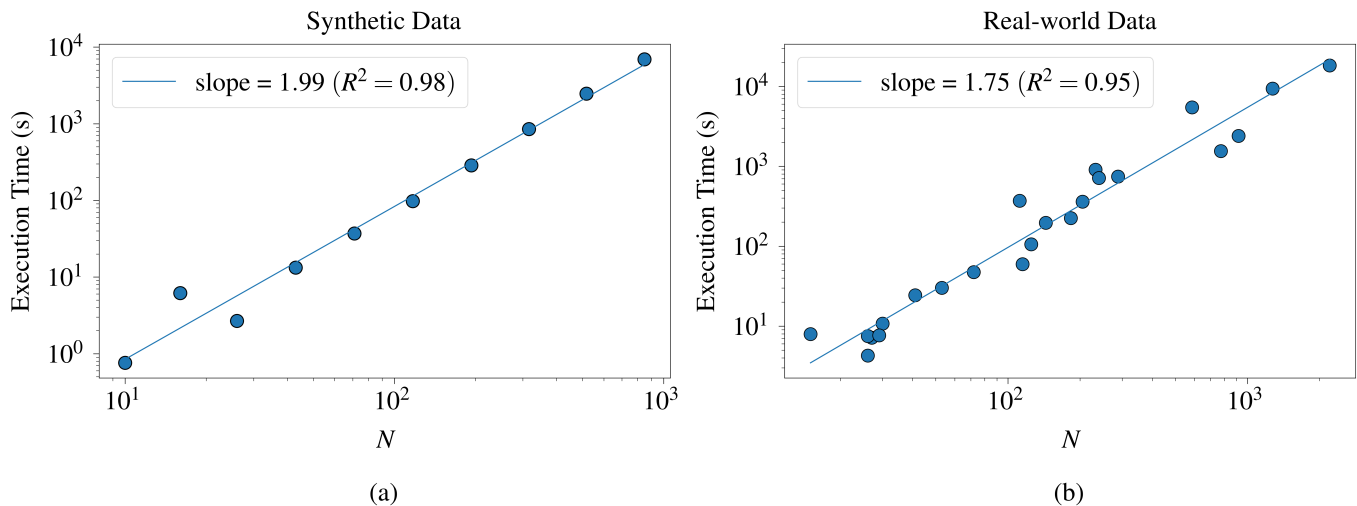


FIG. 6. **Runtime scaling on real and synthetic networks.** (a) Runtimes of the partial rankings algorithm across a set of synthetically generated networks with average degree $\langle k \rangle = 28.5$, showing a quadratic scaling with the network size. (b) Runtimes of the partial rankings algorithm across all empirical networks considered in this study, displaying a scaling of $\sim O(N^{1.75}) < O(N^2)$, with variability attributable to heterogeneity in the edge densities of the real datasets.

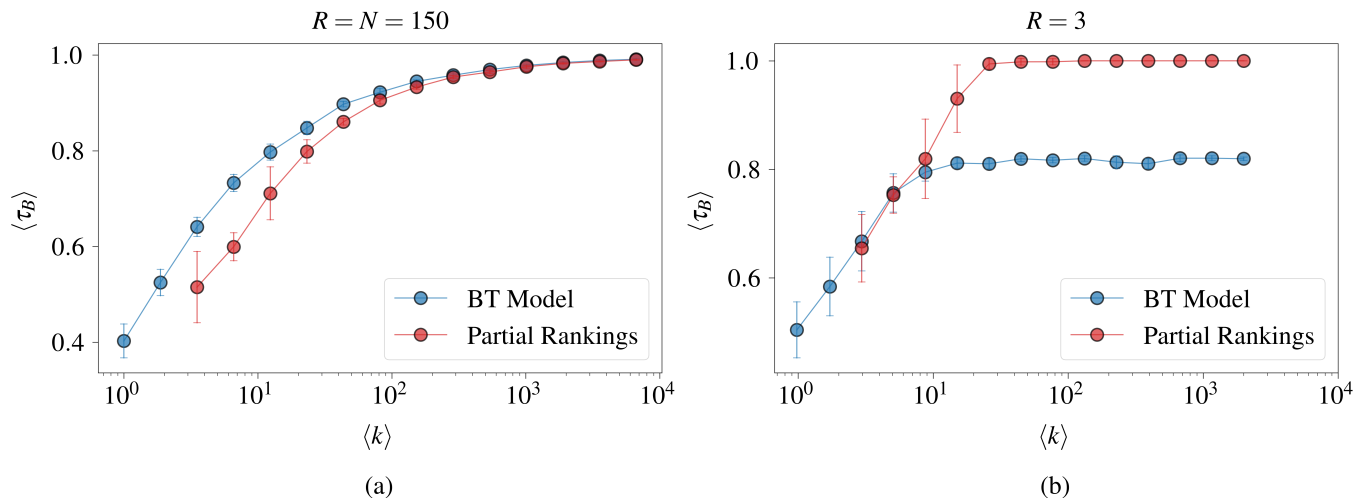


FIG. 7. **Correlations of inferred rankings with planted rankings.** (a) τ_B scores between the rankings inferred by the Bradley-Terry and partial rankings models with respect to the ground truth ranking for the case in which there are no partial rankings ($R = N = 150$). (b) τ_B scores between the rankings inferred by the Bradley-Terry and partial rankings models with respect to the ground truth ranking for the case in which there are three planted partial rankings ($R = 3$). All results are averaged over 10 different simulations and error bars represent 2 standard errors in the mean.

able to reliably recover the correct number of rankings without the need to impose any kind of parameter (such as the bandwidth parameter in mean shift clustering). On the other hand, mean shift clustering is unable to recover the correct number of rankings. When partial rankings are not present (panel (a)), we observe that

neither method is able to recover the correct number of ranks. Crucially, however, our partial rankings algorithm is able to adapt the number of inferred rankings as more evidence becomes available, progressively identifying additional ranks. On the other hand, mean shift clustering remains insensitive to the amount of statistical evidence, consistently inferring approximately the same number of clusters regardless of the number of matches played.

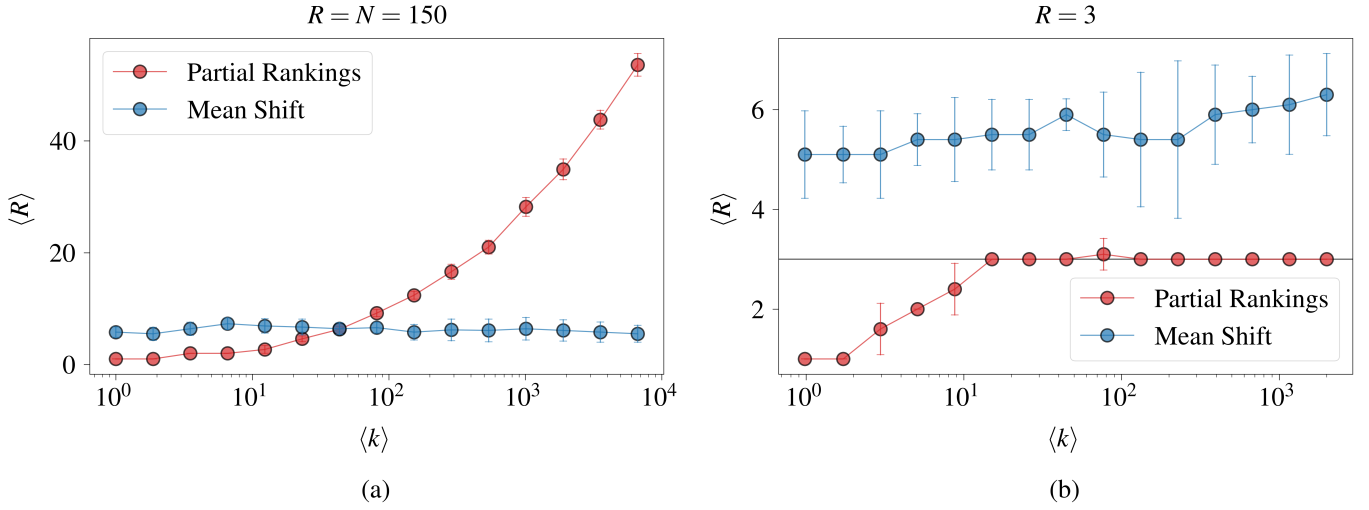


FIG. 8. **Comparison of PR with 1D clustering of BT scores.** (a) Number of ranks inferred by the partial rankings algorithm and mean shift clustering as a function of the average degree of the network for the case where there are no partial rankings ($R = N = 150$). (b) Number of ranks inferred by the partial rankings algorithm and mean shift clustering as a function of the average degree of the network for the case in which there are three planted rankings ($R = 3$, indicated by the solid black line). Results are averaged over 10 different network realisations for each $\langle k \rangle$ value and error bars indicate 2 standard errors in the mean.